Inflammation Vol. 45, No. 4, August 2022 (© 2022)
https://doi.org/10.1007/s10753-022-01641-0

ORIGINAL ARTICLE

Evaluating the Similarity of Different Collagen-Induced Arthritis Models to the Pre-Clinical Phase of RA in Female Rats

Xiaoying Lin[1] , Qiao Wang[1] , Zhixing He[1] , Lin Huang[1] , Chengping Wen[1,3] and Donghai Zhou[2,3]

Received 28 September 2021; accepted 30 January 2022

Abstract— Since the development of RA is a multistep process, it is critical to take action to prevent RA in the pre-clinical phase. Animal models are currently one of the important methods to study RA, but there are very few animal models for studying the pre-clinical phase of RA (Pre-RA). This study aimed to evaluate the similarity of different collagen-induced arthritis models to Pre-RA in rats. Three types of collagen-induced arthritis (CIA) were as follows: (i) standard collagen-induced group (Std-CIA), injected with 200 μg type II collagen at day 0 and 100 μg type II collagen at day 7; (ii) single collagen-induced group (Mono-CIA), injected with 200 μg type II collagen at day 0; (iii) half-dose collagen-induced group (Half-CIA), injected with 100 μg type II collagen at day 0 and 50 μg type II collagen at day 7. Arthritis score, hind paw swelling, serum antibodies, and inflammatory cytokines were measured every 7 days. Gut microbiota analyses were performed on days 0, 11, 21, 28, and 35. Pain threshold measurement, digital radiography, and joint pathology were also assessed. Both Std-CIA and Mono-CIA could successfully cause RA symptoms, including joint swelling and bone erosion, Half-CIA induced only mild swelling in rats. Serum autoantibodies (anti-CCP and anti-CoII) showed no difference among the three types of CIA models, and so did the pain threshold at day 42. In addition, the pathological changes of joint tissues in the Mono-CIA group were the slightest among the collagen-immunized groups. Gut microbiota analysis demonstrated that Half-CIA could impose

Xiaoying Lin and Qiao Wang contributed equally and should be regarded as co-first authors. Chengping Wen and Donghai Zhou contributed equally and should be regarded as co-corresponding authors.

[1]College of Basic Medical Science, Zhejiang Chinese Medical University, Hangzhou 310053, China
[2]Department of Rheumatology, The Second Affiliated Hospital of Zhejiang Chinese Medical University, Hangzhou 310005, China
[3]To whom correspondence should be addressed at and College of Basic Medical Science, Zhejiang Chinese Medical University, Hangzhou, 310053, China. Email: wengcp@163.comDepartment of Rheumatology, The Second Affiliated Hospital of Zhejiang Chinese Medical University, Hangzhou, 310005, China. Email: zhou_donghai@126.com

Abbreviations Pre-RA, Pre-clinical phase of RA; CIA, Collagen-induced arthritis; CCP, Cyclic citrullinated peptide; ACPA, Anticitrullinated protein antibodies; CoII, Type-II collagen; SPF, Specific pathogen-free; H&E, Hematoxylin & eosin; Saf-O/FG, Safranin O/fast green; MPT, Mechanical pain threshold; OUTs, Operational taxonomical units; PCoA, Principal coordinate analysis

similar effects on upregulating genus *Prevotella* as Std-CIA, but Mono-CIA was weaker than them in rats. According to the characteristics of pre-RA, the Half-CIA model is the best suitable animal model for pre-RA among three types of CIA models in rats and can be a valuable model for pre-RA research.

KEY WORDS: Preclinical RA; Animal model; CIA; Gut microbiota; Prevotella

INTRODUCTION

Rheumatoid arthritis (RA) is a chronic and systemic inflammatory disease characterized by synovial inflammation and the progressive destruction of joint cartilage and bones [1]. The onset of RA is much earlier than the clinical diagnosis by current diagnostic criteria, Anticitrullinated protein antibodies (ACPAs) usually appear several years before the onset of RA though not all ACPAs positive individuals progress to RA [2]. The chance of clinically suspected arthralgia (CSA) or undifferentiated arthritis (UA) patients with ACPAs positive progressing to RA within 1 year was found to be 60–70% [3, 4]. This RA high conversion risk time period has been termed " Pre-clinical RA" by many investigators, although lacks unifying definition at present [5]. Based on the current understanding of the etiology, pathological changes of pre-RA are different from RA, and intervention at this stage can change the course of RA [6].

The development of animal models is a prerequisite for screening drugs and revealing pathogenesis in scientific research [7, 8]. The models of RA have been developed in a variety of animal models, which are useful to study the progression and pathogenesis of RA [9]. Arguably the most widely studied animal model of RA has been collagen-induced arthritis. In this model, type-II collagen (CoII), when presented in conjunction with an adjuvant, predictably and reproducibly precipitates chronic inflammatory arthritis in the joints of genetically susceptible animals [10]. However, there is no animal model, which can reflect the features of pre-RA. The major challenge of developing the pre-RA model is to assess the similarity of animal model with the features of pre-RA. In the present study, we used different collagen injection methods to construct collagen-induced models in Wistar rats. To evaluate the similarity of collagen-induced models with the features of pre-RA, this study explored changes in antibodies, joint inflammation, and gut microbiota in rats. As previous literature reported, intestinal dysbiosis may be responsible for changes in innate and adaptive immunity contributing to the development of RA [11, 12]. Our results might provide a suitable pre-RA model for understanding RA development.

MATERIAL AND METHODS

Animal and Study Design

The present study was performed in accordance with the National Institutes of Health Guide for the Care and Use of Laboratory Animals and was approved by the Institutional Animal Care and Use Committee of Zhejiang Chinese Medical. Thirty-two specific pathogen-free (SPF) female Wistar rats (7-week-old) were provided by Shanghai SLAC Laboratory Animal Co., Ltd. After 7 days of acclimatization, all 32 rats were randomly divided into four groups: (1) control group (CT, $n = 8$ rats/group), injected with 0.9% NaCl solution; (2) standard collagen-induced group (Std-CIA, $n = 8$ rats/group), injected with 200 μg type II collagen (in 200 μL incomplete Freund's adjuvant) at day 0 and 100 μg type II collagen (in 100 μL incomplete Freund's adjuvant) at day 7; (3) single collagen-induced group (Mono-CIA, $n = 8$ rats/group), injected with 200 μg type II collagen (in 200 μL incomplete Freund's adjuvant) at day 0; (4) half-dose collagen-induced group (Half-CIA, $n = 8$ rats/group), injected with 100 μg type II collagen (in 100 μL incomplete Freund's adjuvant) at day 0 and 50 μg type II collagen (in 50 μL incomplete Freund's adjuvant) at day 7. Rats were housed in a temperature– and humidity–controlled facility under 12-h light/dark cycle (lights on at 7 am) with access to food and water ad libitum. The study was performed in 42 days.

Type II collagen was dissolved in 0.05 mol/L acetic acid and emulsified with an equal volume of incomplete Freund's adjuvant according to the method described previously [10]. Rats of collagen-induced groups were injected with type II collagen-incomplete Freund's adjuvant at the base of the tail (day 0). On study day 7 after the first initial immunization, rats of CIA and Half-CIA

groups were injected with type II collagen-incomplete Freund's adjuvant at the base of the tail again.

Assessment of Arthritis Severity

The clinical symptoms of arthritis rats, including the arthritis score, hind paw swelling volume, and body weight, were measured every 7 days. The arthritis score was measured with the scores of two hind paws on a total score of 0–8, where each paw was scored as described previously [13]. The hind paws' swelling was quantified by measuring paw volume using a YSC-7C paw volume meter (Shandong Academy of Medical Sciences, Jinan, China). In addition, X-ray images of the right hind paw of three representative rats were obtained to observe joint changes, using CARESTREAM Image Station System (Carestream Health, Inc., USA) to take the radiographs. Mechanical pain threshold (MPT) of the hind paw was tested with five applications of von Frey filaments (Touch Test Sensory Evaluator, North Coast Medical, USA) using the up-and-down method [14], at 42 days after the initial immunization. For histopathological analysis, Rat ankle joints were fixed in 4% formaldehyde for 48 h at 4 ℃ and then were decalcified in EDTA (Servicebio, Wuhan, China) for 4 weeks at 4 °C, with changes of the decalcification solution every 3 to 4 days. Decalcified ankle joints were embedded in paraffin wax by Haoke Bio Inc. Mid-sagittal Sects. (5 μm) of the sections were stained with hematoxylin & eosin (H&E) and Safranin O/fast green (Saf-O/FG).

Measurements of Serum Autoantibodies

On days 7, 14, 21, 28, and 35, blood samples were collected from rats that were anesthetized with diethyl ether, and the samples were centrifuged at 3000 rpm for 15 min at 4 °C to separate the serum. The serum levels of type II collagen antibody (CoII) and anti-cyclic citrullinated peptide antibody (anti-CCP) were evaluated using CUSABIO ELISA Kits (Wuhan, China).

Gut Microbiome Analysis

Stool samples were collected on days 0, 11, 21, 28, and 35 and stored at –80 °C for further analysis. Total genomic DNA was extracted from each stool sample using a stool DNA isolation kit (Tiangen, Biotech Co., Ltd., Beijing, China) according to the manufacturer's protocols. After extraction, DNA concentration and purity were determined using a NanoDrop 2000 spectrophotometer (Thermo Fisher Scientific, USA). Harvested DNA was PCR amplified with broad-range bacterial primers targeting the V3–V4 region of the 16S rRNA gene as previously described [15]. Subsequently, the amplicons were purified according to standard procedures, quantified, pooled, and sequenced with the MiSeq Reagents Kit v3 (600 cycles, Illumina) according to the manufacturer's instructions. The sequencing reaction was conducted by Hangzhou Legenomics Bio-Pharm Technology Co., Ltd., Zhejiang, China.

Sequences were analyzed using Quantitative Insights into Microbial Ecology (QIIME) [16]. High-quality reads were selected and all of the effective reads were clustered into operational taxonomical units (OTUs). The reads with > 97% similarity were assigned to the same OTUs by UCLUST [17]. Bacterial taxonomy was assigned by using the SILVA [18] and NCBI databases [19]. The OTU table was imported into R software and alpha and beta diversity metrics were computed using the "vegan" package. To analyze the alpha diversity, Shannon and Chao1 indices were performed by using R software. For the beta diversity analysis, the principal coordinate analysis (PCoA) based on the unweighted UniFrac distance matrices were visualized by R software. OTUs with > 0.05% mean abundance in one sample and observed in > 10% of the samples were included in differential analyses.

Statistics

All results were presented as Mean ± SEM of data. Each assay comprised at least three biological replicates and each sample was examined with two technical replicates. Differences between groups were evaluated with one-way ANOVA. Statistical analysis was performed using Prism 8.0 (GraphPad Software, USA). Following statistical analyses with multiple comparisons, the p value was adjusted using the Benjamini–Hochberg method to control the false discovery rate (FDR). An adjusted p value of 0.05 was used as a statistically significant cutoff.

RESULTS

Arthritis Score, Paw Swelling, and Body Weight

After injecting type II collagen, signs of arthritis appeared in immunized rats, which were scored and showed by arthritis score and paw volume. As illustrated

in Fig. 1A and B, the collagen injection successfully caused arthritis inflammation, and arthritis severity ranged from high to low in Std-CIA, Mono-CIA, and Half-CIA groups, respectively. Signs of arthritis increased slightly in the Half-CIA group, though there was no significant difference compared to the CT group (Fig. 1B). We plotted Fig. 1C to illustrate the mechanical pain threshold in collagen-immunized groups and controls. Quantitative algetic testing with MPT reveals a decrease in all the three collagen-immunized groups at day 35. Additionally, arthritis inflammation induced the reduction of body weight, and the severity of arthritis inflammation was positively associated with the reduction of body weight in rats (Fig. 1D). There were only statistically significant differences between Mono-CIA, Std-CIA, and CT groups.

In sum, both Std-CIA and Mono-CIA induced severe arthritis inflammation, but Half-CIA induced only mild signs of arthritis and obvious arthralgia in rats.

Arthritis Histopathology

To evaluate inflammation and bone lesions induced by collagen, X-ray was performed. As shown in Fig. 2A, no radiological findings of arthritis were observed in normal joints. After the injection of collagen, the Mono- and Std-CIA groups had the characteristics of arthritic joints, such as joint swelling, joint deformity, bone erosions. However, Half-CIA caused nonvisible bone erosion and soft-tissue swelling in the group (Fig. 2A). Next, we sought to determine the histopathological changes among different groups. H&E staining was used to observe the joint tissue structure. And SOFT staining was used to evaluate the degree of reduction of articular cartilage, in which cartilage is stained to red and bone to green (Fig. 2B). The histopathological examination showed that the CT group had clear joint space and intact articular cartilage; chondrocytes were arranged in neat rows. Std-CIA group observed destroyed joint structure, narrowed

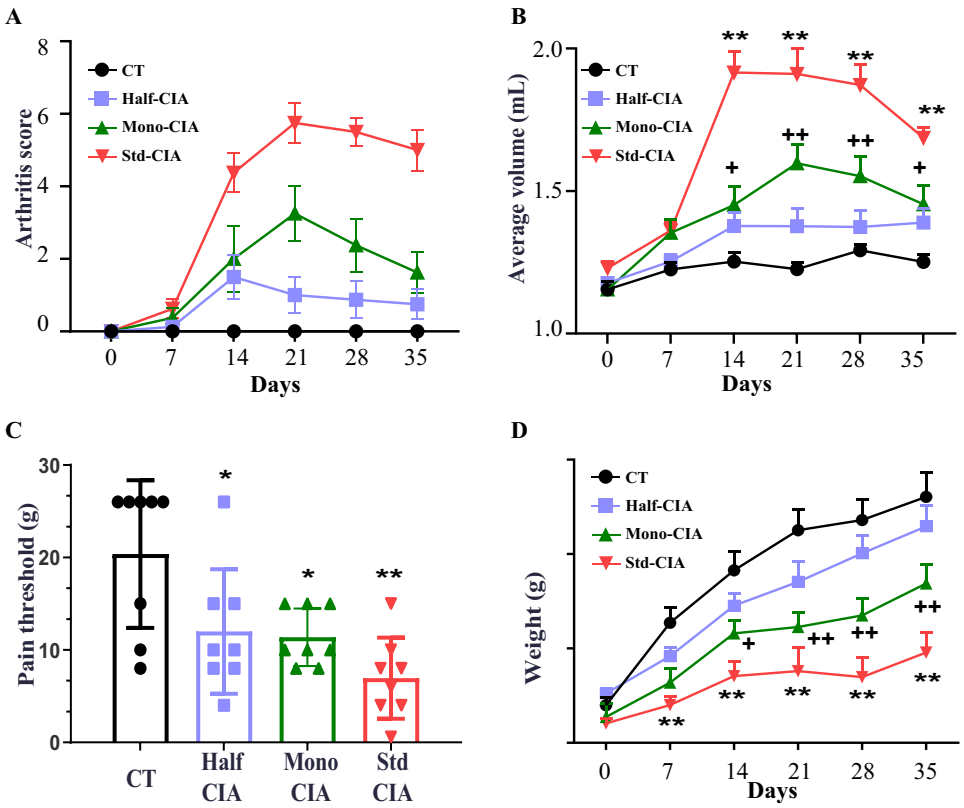

Fig. 1 Alterations in arthritis scores (**A**), volumes (**B**), pain threshold on day 42 (**C**), and weights (**D**) of rats in four groups. "**" represents $p < 0.01$ in the comparison of CT; "++" or "+" represents $p < 0.01$ or $p < 0.05$ in the comparison of CT and Std-CIA, respectively.

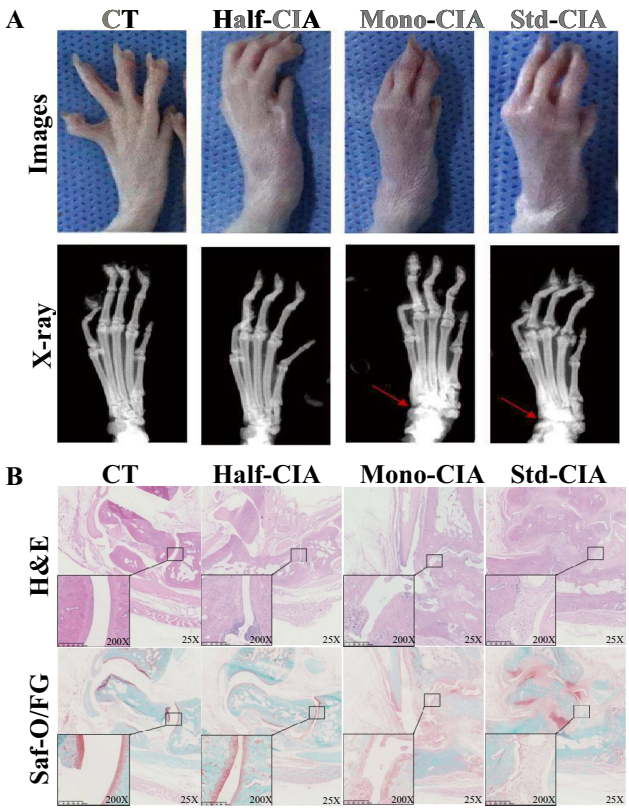

Fig. 2 Representative outline images, X-ray photographs, H&E, and Saf-O/FG staining pictures of joints in rats of four groups.

joint space and H&E staining showed a large amount of inflammatory cell infiltration. Cartilage proteoglycans staining intensity was severely reduced and chondrocytes were significantly reduced and arranged disorderly in some areas. In the Mono-CIA group, infiltration of inflammatory cells in the joint was also observed. SOFT staining showed erosion of articular cartilage and reduction of proteoglycan in this group. Interestingly, articular proteoglycans damage was much milder than that in the Mono-CIA group and the Std-CIA group, although inflammatory cell infiltration was also observed in Mono-CIA group. Overall, the pathological changes of joint tissues in the Mono-CIA group were the slightest among all collagen-immunized groups.

Serum Autoantibodies

As summarized in Fig. 3, serum concentrations of anti-CoII, anti-CCP were evaluated. Starting from day 21, all three CIA groups had remarkably higher serum concentrations of anti-CoII and anti-CCP than the CT group (Fig. 3). Significantly statistical significance was also observed in both CT *vs.* Std-CIA and CT *vs.* Mono-CIA for anti-CoII on days 7 and 14 (Fig. 3). In addition, there were significant differences in anti-CoII on days 28 and 35 between Std-CIA and Half-CIA groups, but no difference between Std-CIA and Mono-CIA. Interestingly, anti-CCP was notably higher in Std-CIA than Mono-CIA on days 21, 28, and 35, but showed no obvious difference in Std-CIA *vs.* Half-CIA.

Alterations of Gut Microbiota in Collagen-Induced Arthritis Rats

Next, we investigated whether there are differences in the gut microbiota in four groups at different time points. First, we integrated the data we obtained on different time points by principal component analysis (PCoA). The clusters of day 35 on the PCoA chart were far away from other clusters, which means that the structure of

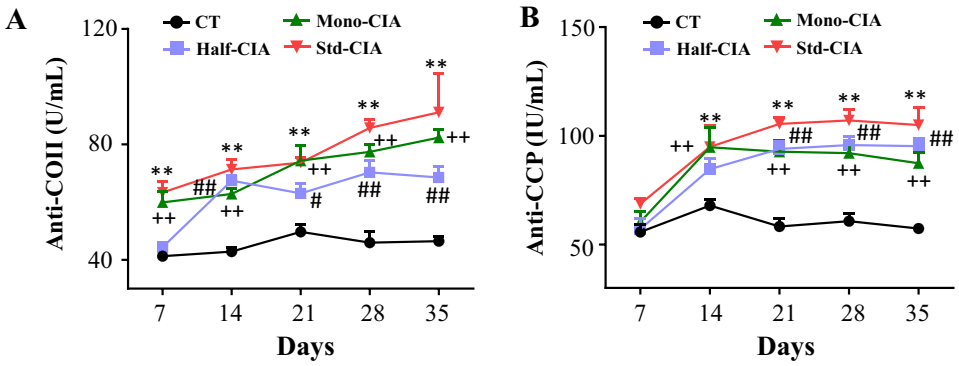

Fig. 3 Dynamic concentrations of serum anti-CoII (**A**) and anti-CCP (**B**) in rats of four groups. "**" represents $p < 0.01$ in the comparison of CT and Std-CIA; "++" represents $p < 0.01$ in the comparison of CT and Std-CIA. "##" or "#" represents $p < 0.01$ or $p < 0.05$ in the comparison of CT and Mono-CIA, respectively.

day 35's microbial community was quietly different from other clusters (Fig. 4A). Then we assessed the average phylum-level bacteria composition from feces. The highest relative abundance of bacteria was *Firmicutes*, followed by *Bacteroides* in each group at all time points. On day 35, the relative abundance of *Proteobacteria* in Std-CIA was markedly decreased, compared with the CT group (Fig. 4B).

Previous literature has reported that the enrichment of *Prevotella* sp. in individuals was found in the pre-clinical stages of RA. Hence, this study showed the dynamic alterations of genus *Prevotella* in CIA rats. There were five subgroups of genus *Prevotella* being observed in the CIA rats, including *Prevotella*, *Prevotella*_1, *Prevotella*_2, *Prevotella*_7, and *Prevotella*_9. During the development of the rats, *Prevotella*, *Prevotella*_2, and *Prevotella*_7 showed the increasing trends, but the *Prevotella*_1 and *Prevotella*_9 showed the decreasing trends (Fig. 5). On day 35, *Prevotella*, *Prevotella*_2 had significantly higher abundance in Half-CIA and Std-CIA compared to CT (Fig. 5). Additionally, Half-CIA and Std-CIA caused the significant upregulation of *Prevotella*_1 (Fig. 5). In sum, the Half-CIA and Std-CIA showed similar effects on the regulation of genus *Prevotella*.

DISCUSSION

Recently, new aspiration emerges to cure and even prevent RA, shifting the "window of opportunity" to the pre-clinical phases of RA [20]. However, currently used RA animal models are established to mimic

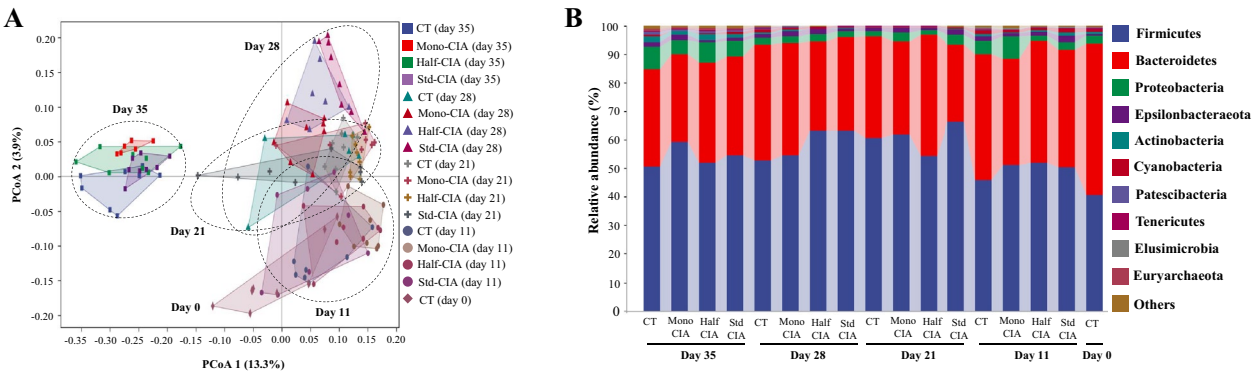

Fig. 4 (**A**) PCoA scores based on unweighted UniFrac distance of gut microbiota. (**B**) Relative percentage abundance of the identified phylum of rats in four groups.

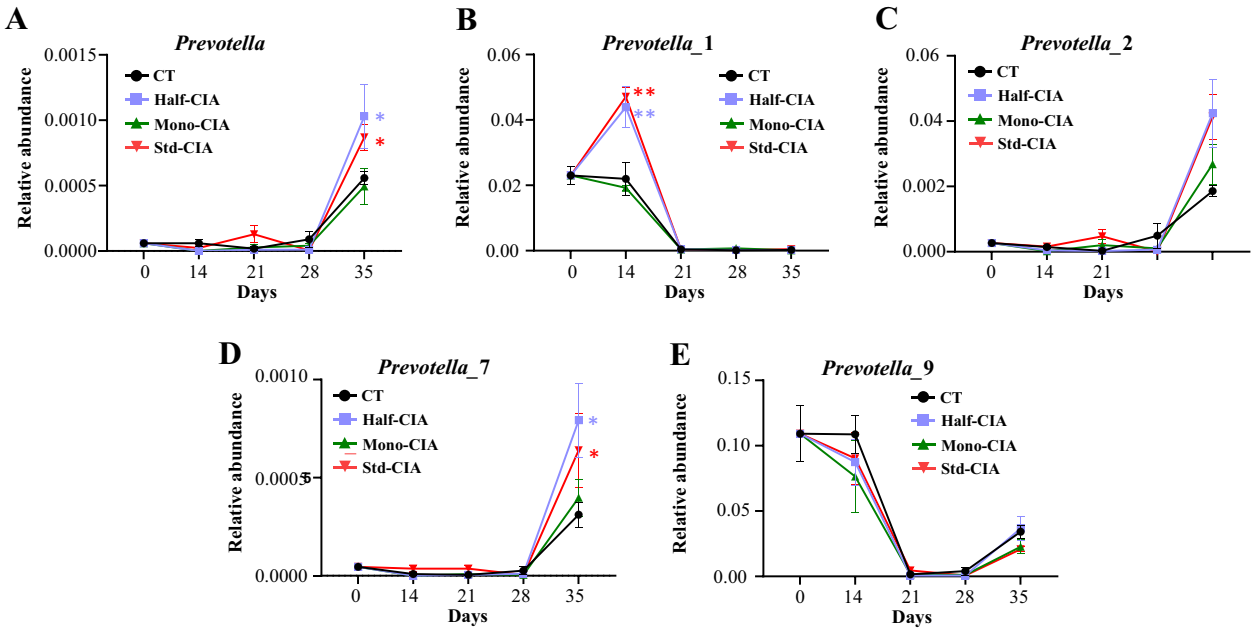

Fig. 5 Dynamic relative abundance of genus *Prevotella*. (**A**) *Prevotella*; (**B**) *Prevotella*_1; (**C**) *Prevotella*_2; (**D**) *Prevotella*_7; (**E**) *Prevotella*_9. "**" or "*" represents $p < 0.01$ or $p < 0.05$ in the comparison of CT and Std-CIA, respectively.

characteristics of clinically diagnosed RA; there is no dedicated animal model for pre-RA, which limited the understanding of pre-RA. An ideal pre-RA model should be able to fully replicate the characteristics of this period, including pathogenesis, clinical symptoms, serological indicators, and disease prognosis, etc.

Adjuvant arthritis (AA) and type II collagen-induced arthritis (CIA) models are the most widely used induced models in RA research. Compared with AA, CIA is induced by homologous tissues, and CIA lesions are chronic proliferative synovitis and will cause the destruction of articular cartilage and synovium, while the AA model lacks chronic process, cartilage destruction is mild and bone destruction is more serious. Therefore, this study was designed to replicate the pre-RA method based on the CIA model and evaluate its similarity to the pre-RA state according to the methodology introduced in the ref [21].

Based on the indicators of autoantibodies, arthritis inflammation, joint destruction and gut microbiota, this study successfully found a construction method of Pre-RA in female Wistar rats. Peptidyl arginine deiminases (PADs) convert arginine residues in vimentin and type II collagen peptide chains into citrulline residues, which creates autoantigenic B cell epitopes [22]. The antibodies produced by B cells against these epitopes are called ACPA. Anti-CCP and anti-CoII antibodies can be found in individuals before symptom onset [23]. Therefore, the ACPA-positive is one of the essential indices for defining Pre-RA. In the present study, serum anti-CoII and anti-CCP antibody were significantly upregulated by collagen in all three types of CIA models. Another important index of defining Pre-RA is the nonspecific symptoms including arthralgia and mild joint swelling. Based on arthritis symptoms including joint swelling, paw pain threshold, joint erosion, this study demonstrated that above RA symptoms were present in Std-CIA and Mono-CIA, except no obvious joint swelling and erosion in Half-CIA in rats. In addition, pain threshold and joint pathology showed that characteristics of pre-RA still exist at day 35, although the CIA model may represent spontaneous remission over time.

Recent studies have suggested that the initial steps of the pathological autoimmune response may originate in mucosal sites, rather than in the joints [24]. Intestinal dysbiosis plays a causal role in the pathogenesis of RA and promotes the development of arthritis in CIA-induced mice [25, 26]. The key gut microbiota association in RA

patients is the relative increase in the abundance of *Prevotella* sp., particularly *Prevotella copri* (*P. copri*), which presents early in the course of RA [27]. In addition, *P. copri* is also positively associated with clinical parameters of RA patients, further supporting its pathophysiological relevance to the disease [28]. This study successfully observed five subgroups of *Prevotella* spp. in CIA rats, including *Prevotella*, *Prevotella*_1, *Prevotella*_2, *Prevotella*_7, and *Prevotella*_9. Among three types of CIA models, Half-CIA and Std-CIA almost follow the same changing trends in the five subgroups of *Prevotella* sp. Therefore, the dynamic alterations of *Prevotella* sp. further demonstrated that the Half-CIA model could imitate the characteristics of "Pre-CIA" in rats.

In summary, the Half-CIA successfully induced the ACPA-positive and the increase of *Prevotella* sp. in rats but cause mild signs of inflammation, which are characteristics of pre-RA. And though given only half-dose Col II, ACPAs and inflammatory signs were still present at day 35. To our knowledge, this study is the first to report the Pre-RA model, which will be useful for us to better understand the pathology of Pre-RA and screen drugs for Pre-RA treatment. However, this study also had several limitations. More indicators are needed to assess the similarity of the Pre-RA models to patients.

CONCLUSION

According to the characteristics of pre-RA, the Half-CIA model is the best suitable animal model for pre-RA among three types of CIA models in rats and can be a valuable model for pre-RA research.

AUTHOR CONTRIBUTION

ZH and CW conceived of and proposed the idea, designed the study. XL and DZ performed the experiment. ZH and LH participated in data analysis. QW revised the figures and made great contribution to the revision. DZ and ZH contributed to writing assistance and reading and revising the manuscript. All authors read and approved the final manuscript.

FUNDING

This work was supported by the National Key R&D Program of China (2018YFC1705500) & Foundation of Zhejiang Chinese Medicine University (2021ZZ01).

AVAILABILITY OF DATA AND MATERIALS

The datasets used in this study are available from the corresponding author on valid request.

DECLARATIONS

Ethics Approval and Consent to Participate All animal handling and experimental procedures were performed in accordance with local ethical committees and the National Institutes of Health Guide for the Care and Use of Laboratory Animals. All efforts were made to minimize animal suffering and to reduce the number of animals used. All procedures performed in this study involving animals were approved by the ethics committee of our university.

Consent for Publication Not applicable.

Competing Interests The authors declare no competing interests.

REFERENCES

1. Müller-Ladner, U., T. Pap, R.E. Gay, M. Neidhart, and S. Gay. 2005. Mechanisms of disease: The molecular and cellular basis of joint destruction in rheumatoid arthritis. *Nature Clinical Practice Rheumatology* 1 (2): 102–110.
2. Tilvawala, R., S.H. Nguyen, A.J. Maurais, V.V. Nemmara, M. Nagar, A.J. Salinger, S. Nagpal, E. Weerapana, and P.R. Thompson. 2018. The rheumatoid arthritis-associated citrullinome. *Cell Chemical Biology* 25 (6): 691–704.e6.
3. Chatzidionysiou, K., E. Lie, G. Lukina, M.L. Hetland, E.-M. Hauge, K. Pavelka, C. Gabay, A. Scherer, D. Nordström, H. Canhao, et al. 2017. Rituximab retreatment in rheumatoid arthritis in a real-life cohort: Data from the CERERRA collaboration. *Journal of Rheumatology* 44 (2): 162–169.
4. van Steenbergen, H.W., J.A.P. da Silva, T.W.J. Huizinga, and A.H.M. van der Helm-van Mil. 2018. Preventing progression from arthralgia to arthritis: Targeting the right patients. *Nature Reviews Rheumatology* 14 (1): 32–41.
5. Mankia, K., and P. Emery. 2016. Preclinical rheumatoid arthritis: Progress toward prevention. *Arthritis & Rhematology* 68 (4): 779–788.
6. van Nies, J.A.B., R. Tsonaka, C. Gaujoux-Viala, B. Fautrel, and A.H.M. van der Helm-van Mil. 2015. Evaluating relationships between symptom duration and persistence of rheumatoid arthritis: Does a window of opportunity exist? Results on the Leiden early arthritis clinic and ESPOIR cohorts. *Annals of the Rheumatic Diseases* 74 (5): 806–812.
7. Zhang, C., W. Zhang, R. Shi, B. Tang, and S. Xie. 2019. extract ameliorates inflammation and oxidative stress in a complete Freund's adjuvant-induced rheumatoid arthritis model. *Pharmaceutical Biology* 57 (1): 792–798.

8. Guo, C., R. Fu, S. Wang, Y. Huang, X. Li, M. Zhou, J. Zhao, and N. Yang. 2018. NLRP3 inflammasome activation contributes to the pathogenesis of rheumatoid arthritis. *Clinical and Experimental Immunology* 194 (2): 231–243.
9. Choudhary, N., L.K. Bhatt, and K.S. Prabhavalkar. 2018. Experimental animal models for rheumatoid arthritis. *Immunopharmacology and Immunotoxicology* 40 (3): 193–200.
10. Rosloniec, E.F., M. Cremer, A.H. Kang, L.K. Myers, and D.D. Brand. 2010. Collagen-induced arthritis. *Current Protocols Immunology* Chapter 15 :Unit 15.15.11-Unit 15.525.
11. Horta-Baas, G., M.D.S. Romero-Figueroa, A.J. Montiel-Jarquín, M.L. Pizano-Zárate, J. García-Mena, and N. Ramírez-Durán. 2017. Intestinal dysbiosis and rheumatoid arthritis: A link between gut microbiota and the pathogenesis of rheumatoid arthritis. *Journal of Immunology Research* 2017: 4835189.
12. Jiao, Y., L. Wu, N.D. Huntington, and X. Zhang. 2020. Crosstalk between gut microbiota and innate immunity and its implication in autoimmune diseases. *Frontiers in Immunology* 11: 282.
13. Mossiat, C., D. Laroche, C. Prati, T. Pozzo, C. Demougeot, and C. Marie. 2015. Association between arthritis score at the onset of the disease and long-term locomotor outcome in adjuvant-induced arthritis in rats. *Arthritis Research & Therapy* 17: 184.
14. Pitcher, G.M., J. Ritchie, and J.L. Henry. 1999. Paw withdrawal threshold in the von Frey hair test is influenced by the surface on which the rat stands. *Journal of Neuroscience Methods* 87 (2): 185–193.
15. Yu, Y., Q. Liu, H. Li, C. Wen, and Z. He. 2018. Alterations of the gut microbiome associated with the treatment of hyperuricaemia in male rats. *Frontiers in Microbiology* 9: 2233.
16. Caporaso, J.G., J. Kuczynski, J. Stombaugh, K. Bittinger, F.D. Bushman, E.K. Costello, N. Fierer, A.G. Peña, J.K. Goodrich, J.I. Gordon, et al. 2010. QIIME allows analysis of high-throughput community sequencing data. *Nature Methods* 7 (5): 335–336.
17. Edgar, R.C. 2010. Search and clustering orders of magnitude faster than BLAST. *Bioinformatics* 26 (19): 2460–2461.
18. Quast, C., E. Pruesse, P. Yilmaz, J. Gerken, T. Schweer, P. Yarza, J. Peplies, and F.O. Glöckner. 2013. The SILVA ribosomal RNA gene database project: improved data processing and web-based tools. *Nucleic Acids Research* 41 (Database issue): D590-D596.
19. Sayers, E.W., R. Agarwala, E.E. Bolton, J.R. Brister, K. Canese, K. Clark, R. Connor, N. Fiorini, K. Funk, T. Hefferon, et al. 2019. Database resources of the National Center for Biotechnology Information. *Nucleic Acids Research* 47 (D1): D23–D28.
20. Petrovská, N., K. Prajzlerová, J. Vencovský, L. Šenolt, and M. Filková. 2021. The pre-clinical phase of rheumatoid arthritis: from risk factors to prevention of arthritis. *Autoimmunity Reviews* 20 (5): 102797.
21. van der Staay, F.J., S.S. Arndt, and R.E. Nordquist. 2009. Evaluation of animal models of neurobehavioral disorders. *Behavioral and Brain Functions* 5: 11.
22. Schellekens, G.A., B.A. de Jong, F.H. van den Hoogen, L.B. van de Putte, and W.J. van Venrooij. 1998. Citrulline is an essential constituent of antigenic determinants recognized by rheumatoid arthritis-specific autoantibodies. *The Journal of Clinical Investigation* 101 (1): 273–281.
23. Willemze, A., L.A. Trouw, R.E.M. Toes, and T.W.J. Huizinga. 2012. The influence of ACPA status and characteristics on the course of RA. *Nature Reviews Rheumatology* 8 (3): 144–152.
24. Brusca, S.B., S.B. Abramson, and J.U. Scher. 2014. Microbiome and mucosal inflammation as extra-articular triggers for rheumatoid arthritis and autoimmunity. *Current Opinion in Rheumatology* 26 (1): 101–107.
25. Jubair, W.K., J.D. Hendrickson, E.L. Severs, H.M. Schulz, S. Adhikari, D. Ir, J.D. Pagan, R.M. Anthony, C.E. Robertson, D.N. Frank, et al. 2018. Modulation of Inflammatory Arthritis in Mice by Gut Microbiota Through Mucosal Inflammation and Autoantibody Generation. *Arthritis & Rhematology* 70 (8): 1220–1233.
26. Peng, J., X. Lu, K. Xie, Y. Xu, R. He, L. Guo, Y. Han, S. Wu, X. Dong, Y. Lu, et al. 2019. Dynamic alterations in the gut microbiota of collagen-induced arthritis rats following the prolonged administration of total glucosides of paeony. *Frontiers in Cellular and Infection Microbiology* 9: 204.
27. Alpizar-Rodriguez, D., T.R. Lesker, A. Gronow, B. Gilbert, E. Raemy, C. Lamacchia, C. Gabay, A. Finckh, and T. Strowig. 2019. Prevotella copri in individuals at risk for rheumatoid arthritis. *Annals of the Rheumatic Diseases* 78 (5): 590–593.
28. Wells, P.M., A.S. Adebayo, R.C.E. Bowyer, M.B. Freidin, A. Finckh, T. Strowig, T.R. Lesker, D. Alpizar-Rodriguez, B. Gilbert, B. Kirkham, et al. 2020. Associations between gut microbiota and genetic risk for rheumatoid arthritis in the absence of disease: A cross-sectional study. *The Lancet Rheumatology* 2 (7): e418–e427.